1-13-2017

Neutral and Cationic Bis-Chelate Monoorganosilicon(IV) Complexes of 1-Hydroxy-2-pyridinone

James Koch
jgk00615@sjfc.edu

William W. Brennessel
University of Rochester

Bradley M. Kraft
St. John Fisher College, bkraft@sjfc.edu

Publication Information

Koch, James; Brennessel, William W.; and Kraft, Bradley M. (2017). "Neutral and Cationic Bis-Chelate Monoorganosilicon(IV) Complexes of 1-Hydroxy-2-pyridinone." *Organometallics* 36.3, 594-604.

Neutral and Cationic Bis-Chelate Monoorganosilicon(IV) Complexes of 1-Hydroxy-2-pyridinone

Abstract

A series of spirocyclic monoorganosilicon compounds of the form $RSi(OPO)_2Cl$ [R = phenyl (**1**); *p*-tolyl (**2**); benzyl (**3**); Me (**4**); ^{t}Bu (**5**); thexyl (**6**)] (OPO = 1-oxo-2-pyridinone) was synthesized and characterized by ^1H, ^{13}C, and ^{29}Si NMR spectroscopy, X-ray crystallography, and elemental analysis. In the solid state, complexes **1**, **2**, and **3** are neutral and possess *cis*-OPO ligands in an octahedral arrangement, and complexes **4**, **5**, and **6** are cationic and possess effectively *trans*-OPO ligands in nearly ideal square pyramidal geometries along the Berry-pseudorotation coordinate. In **4**-**6**, chloride dissociation is attributed to the additive effect of multiple intermolecular C—H•••Cl interactions in their crystals. In DMSO-d_6 solution, compounds **1**-**6** form cationic hexacoordinate DMSO adducts with *trans*-OPO ligands, all of which undergo dynamic isomerization with energy barriers of ~18-19 kcal/mol. Compounds with better leaving groups, (*p*-tolyl)$Si(OPO)_2X$ [X = I (**7**); X = triflate (**8**)], exhibit identical solution NMR spectra as **2**, supporting anion dissociation in each. The fluoride derivatives $RSi(OPO)_2F$ [R = benzyl (**9**); Me (**10**)] exhibit hexacoordinate geometries with *cis*-OPO ligands in the solid state and exhibit dynamic isomerization in solution. Overall, these studies indicate, in both the solid and solution states, that the *trans*-OPO ligand arrangement is favored when anions are dissociated and a *cis*-OPO ligand arrangement when anions are coordinated.

Keywords

fsc2017

Disciplines

Chemistry

Neutral and Cationic Bischelate Monoorganosilicon(IV) Complexes of 1-Hydroxy-2-Pyridinone

James G. Koch, William W. Brennessel[‡] and *Bradley M. Kraft**[,†]

[†] *Department of Chemistry, St. John Fisher College, Rochester, NY 14618, USA*
[‡] *Department of Chemistry, University of Rochester, Rochester, NY 14627, USA*

Abstract. A series of spirocyclic monoorganosilicon compounds of the form $RSi(OPO)_2Cl$ [R = phenyl (**1**); *p*-tolyl (**2**); benzyl (**3**); Me (**4**); ^{t}Bu (**5**); thexyl (**6**)] (OPO = 1-oxo-2-pyridinone) was synthesized and characterized by ^1H , ^{13}C, and ^{29}Si NMR spectroscopy, X-ray crystallography, and elemental analysis. In the solid state, complexes **1**, **2**, and **3** are neutral and possess *cis*-OPO ligands in an octahedral arrangement, and complexes **4**, **5**, and **6** are cationic and possess effectively *trans*-OPO ligands in nearly ideal square pyramidal geometries along the Berry-pseudorotation coordinate. In **4-6**, chloride dissociation is attributed to the additive effect of multiple intermolecular C—H···Cl interactions in their crystals. In DMSO-d_6 solution, compounds **1**-**6** form cationic hexacoordinate DMSO adducts with *trans*-OPO ligands, all of which undergo dynamic isomerization with energy barriers of ~18-19 kcal/mol. Compounds with better leaving groups, (*p*-tolyl)$Si(OPO)_2X$ [X = I (**7**); X = triflate (**8**)], exhibit identical solution NMR spectra as **2**, supporting anion dissociation in each. The fluoride derivatives $RSi(OPO)_2F$ [R = benzyl (**9**); Me (**10**)] exhibit hexacoordinate geometries with *cis*-OPO ligands in the solid state and exhibit dynamic isomerization in solution. Overall, these studies indicate, in both the solid and solution states, that the *trans*-OPO ligand arrangement is favored when anions are dissociated and a *cis*-OPO ligand arrangement when anions are coordinated.

Introduction. Structural, bonding, and reactivity studies of hypercoordinate organosilicon complexes have been explored extensively and continue to be an active area of interest.[1,2] In organic synthesis, neutral and charged donor-atom complexes of this type are important mediators in carbon-carbon bond forming reactions. In these reactions, the silicon atom acts as the reactive site, and upon expansion of its coordination shell, both its Lewis acidity and reactivity of its carbon substituent as a nucleophile are enhanced. Addition reactions to carbonyl compounds, for example, are often promoted by coordination of neutral Lewis bases such as formamides, sulfoxides, phosphine oxides, and their chiral analogs.[3]

Complexes with expanded coordination spheres also serve as models of intermediates and transition states in the mechanisms of substitution processes at tetracoordinate silicon.[1] Pentacoordinate silicon complexes often manifest geometrical and stereochemical flexibility with low energy barriers to isomerization. The large number of pentacoordinate silicon complexes in the Cambridge Structural Database[4] reveals most, if not all, molecular shapes falling along the Berry-pseudorotation continuum between ideal trigonal bipyramidal (TBP) and square pyramidal (SP) geometries.[5] Significant variations in molecular shape along this continuum have been observed between crystalline forms of the same compound,[6] and even within the same crystal of the same compound,[7] of which were attributed to underlying crystal packing effects.

Previous reports of pentacoordinate organosilicon complexes relevant to the present work have a Si*CO*$_4$ ligand framework for which most fall into the category of zwitterionic spirocyclic organosilicates.[1a] According to the valence-bond model, these complexes can be described as having a formal negative charge on silicon which is charge-balanced by a pendant ammonium group. Cationic complexes having Si*CO*$_4$ cores are comparatively rare in the literature with these and related heteroatom examples arising upon dissociation of halide (X) in RSiL$_2$X complexes bearing an alkyl or aryl R group and two monoanionic bidentate ligands (L). The most abundant and well-studied examples of this type include those of tunable hydrazide-based ligands with an entire series of papers published on their characteristics and behavior.[8] In their reports, the use of ligands with sufficient electron-donating ability has been established as an important factor in promoting anion dissociation. Other reports of this type currently include those based on oxinate,[9] 2-acylpyrrole,[10] salicylaldimine or salen-type,[11] pyridine-2-thiolate,[12] 1,3-diketonate,[13] tropolone,[14] among others,[15,16] not all of which have been observed or probed for their ionization behavior.

We recently reported on the chelation equilibria of neutral di- and triorganosilicon(IV) complexes bearing the 1-oxo-2-pyridinone (OPO) ligand.[17] According to the valence bond model, a chelated OPO ligand adopts a formal positive charge and places a formal negative charge on silicon upon π-electron delocalization in the pyridine ring, and this parallels the electronic effect of the zwitterionic organosilicates (Figure 1).[1a,18] The neutral diorgano complexes, R$_2$Si(OPO)$_2$, readily undergo non-ionic dissociation of their Si←OC dative bonds concomitant with isomerization which is facilitated by increasing temperature, increasing core

ligand sterics, and the influence of hydrogen-bonding donors. As a logical extension of our work, this report describes a new series of monoorgano complexes of the general formula $RSi(OPO)_2X$. The decrease in the number of R groups attached to silicon results in profound differences in the structure and bonding of these complexes, particularly in that they do not show evidence for Si←OC bond dissociation in solution, but instead, in the case of the weakly-coordinating X groups, form silylium ions that are stabilized by coordination of DMSO solvent. The steric and electronic nature of R has surprisingly little effect on the geometry of the formed cations with the two *cis*-OPO ligands in the neutral complexes reorienting effectively to *trans* upon formation of the silylium ions and the resulting molecular shapes all lying on the far limit along the TBP→SP Berry pseudorotation coordinate.

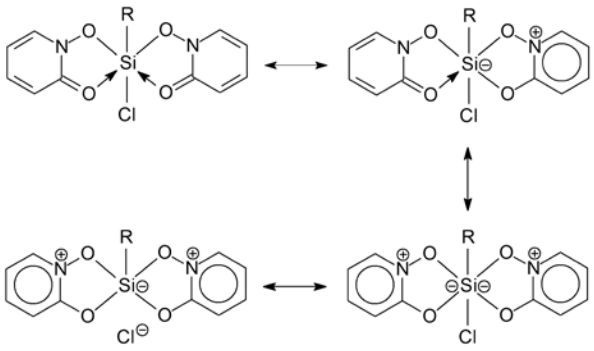

Figure 1. Resonance forms of $RSi(OPO)_2Cl$ complexes.

Synthesis. Monoarylated and monoalkylated complexes of the form $RSi(OPO)_2Cl$ [R = Ph (**1**), *p*-tolyl (**2**), benzyl (Bn) (**3**), Me (**4**), ^{t}Bu (**5**), thexyl (**6**)] were prepared by transsilylation using 2 equiv. of $Me_3Si(OPO)$ with the corresponding trichlorosilane at room temperature with isolated yields ranging from 64-90% (eq 1). Due to their very low solubility in chloroform, acetonitrile, ethereal, and hydrocarbon solvents, all complexes were only able to be characterized in DMSO-d_6 solution by NMR spectroscopy. X-ray quality crystals of each complex were obtained by mixing dilute solutions of each reagent in an appropriate solvent and allowing to stand from several hours to days at room temperature, or were otherwise formed as fine white precipitates under more concentrated conditions. An attempt to prepare $Si(OPO)_2Cl_2$ by the reaction of $SiCl_4$ with 2 equiv. of $Me_3Si(OPO)$ in acetonitrile resulted in the isolation of the well-known stable trischelate, $[Si(OPO)_3]^+Cl^-$.[19]

Solid-state structures. The X-ray crystal structures containing **1**, **2**, and **3** are shown in Figures 2, 3, and 4. Selected bond distances and angles are given in Table 1. All three complexes exhibit distorted octahedral geometries with *cis*-OPO bidentate ligands.[20] Both of the OPO ligands in each complex exhibit C/N site disorder and this gives rise to four possible diastereomers. The disorder ratios suggest a slightly greater probability for the O(N)-*trans*-O(N) arrangement in all three complexes (see Experimental Section). The OPO ligands chelate more strongly in **1-3** (bite angles ~85-86°) than in the related neutral diorgano complexes, $R_2Si(OPO)_2$ [R = Me, Et, ^{i}Pr, Ph], (bite angles ~82-83°),[17] likely due to decreased steric crowding around Si and decreased electron-donation by only one R group. Each O_2Si chelate ring and associated OPO ligand are nearly coplanar forming fold angles of 1.10(11)° and 4.96(8)° in **1**, 0.96(12)° and 3.49(15)° in **2**, and 6.72(6)° and 8.91(5)° in **3**. In **1**, **2**, and **3**, the Si—Cl distances are all ~2.25 Å. There are currently no other crystallographically characterized hexacoordinate complexes with Si*CO*$_4$*X* (*X* = halide) ligand cores. Of the 13 known complexes having Si*CClN*$_2$*O*$_2$ frameworks, four have dissociated chloride ions[21] and nine have Si—Cl bonds ranging from 2.188-2.384 Å.[22]

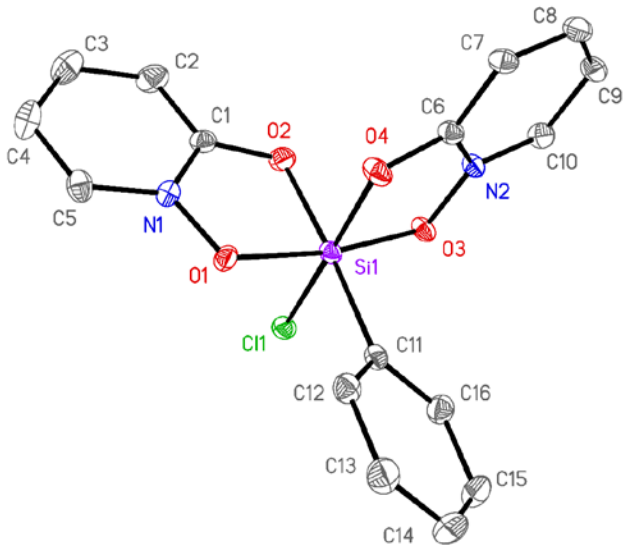

Figure 2. Thermal ellipsoid plot of **1** at the 50% probability level with hydrogen atoms omitted.

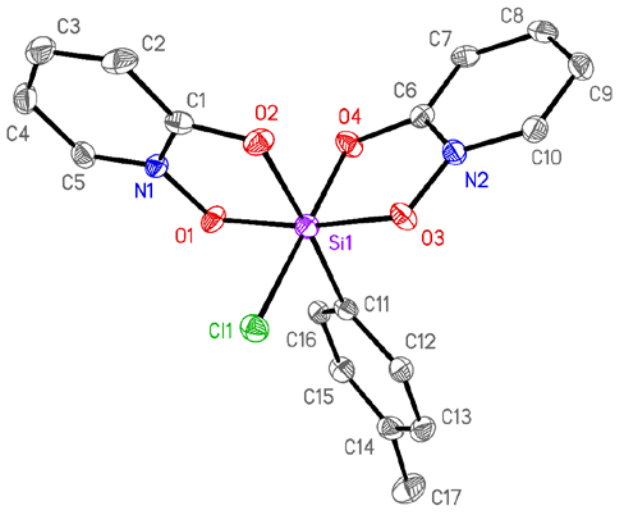

Figure 3. Thermal ellipsoid plot of **2** at the 50% probability level with hydrogen atoms omitted.

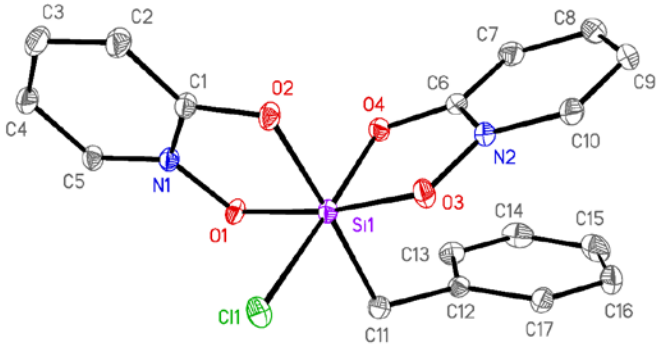

Figure 4. Thermal ellipsoid plot of **3** at the 50% probability level with hydrogen atoms omitted.

Table 1. Selected Bond Distances (Å) and Angles (°) for **1**, **2**, **3**, **9**, and **10**. None of the C-N, N-O, and C-O bond lengths can be represented accurately due to C/N site disorder.

	1	**2**	**3**	**9**	**10**
Si1-O1	1.7876(16)	1.781(2)	1.7984(8)	1.8048(18)	1.8060(15)
Si1-O2	1.8473(16)	1.838(2)	1.8253(8)	1.8797(18)	1.8828(17)
Si1-O3	1.7934(16)	1.790(2)	1.8038(8)	1.8061(19)	1.8120(15)
Si1-O4	1.8311(16)	1.824(2)	1.8307(8)	1.8830(19)	1.8752(16)
Si1-Cl1/F1	2.2457(9)	2.2586(11)	2.2540(4)	1.6597(16)	1.6609(15)
Si1-C11	1.910(2)	1.913(3)	1.9265(10)	1.924(3)	1.887(2)
O1-Si1-O3	170.63(7)	170.49(10)	171.18(4)	169.46(8)	167.03(7)
O2-Si1-C11	176.05(8)	176.25(12)	176.96(4)	172.90(10)	174.90(8)
O4-Si1-Cl1/F1	172.45(6)	172.91(8)	173.37(3)	169.84(9)	169.31(7)
O1-Si1-O2	85.04(7)	85.17(10)	85.42(3)	84.09(8)	83.77(6)
O3-Si1-O4	86.28(7)	86.36(10)	86.40(3)	84.61(8)	84.57(6)
O2-Si1-O3	86.17(7)	85.93(10)	86.19(4)	86.52(8)	85.35(7)
O2-Si1-O4	87.43(7)	88.17(10)	87.65(4)	86.02(8)	84.88(8)
O1-Si1-O4	90.11(7)	90.01(10)	90.56(3)	89.96(8)	87.46(7)
C11-Si1-Cl1/F1	92.95(7)	92.12(9)	91.41(3)	95.81(10)	95.84(9)

In contrast with **1**-**3**, complexes **4-6** crystallize as ion pairs (Figures 5, 6, and 7) and exhibit remarkably similar structures in light of large differences in the sterics of the alkyl groups. All three structures exhibit a nearly ideal square pyramidal (SP) geometry[23] with the alkyl group occupying the apical position, the OPO ligands situated effectively *trans* to each other, and the chloride ion located nearly linearly opposite of the alkyl ligand off of the vacant coordination site at a distance of ~3.5 Å. Selected bond distances and angles are given in Table 2. Although primarily ionic bonding is evident, the consistent and regular positions of the chloride ions in the silicon coordination spheres and the Si—Cl distances less than the sum of the van der Waals radii of 3.85 Å[24] suggest the possibility of a minor component of Si—Cl covalent bonding character in each. In **4-6**, their OPO-ligand disordered structures indicate the presence of two possible isomers, O(N)-*trans*-O(N) and O(N)-*trans*-O(C), with the disorder ratios indicating a slightly greater probability for the latter in each (see Experimental Section). The OPO ligand bite angles in **4-6** (~87°) are larger than those in **1-3** (~85-86°) and indicate a stronger binding affinity as a likely consequence of the greater electrophilicity of the formed cations, and are comparable to those of the trischelate cation, $[Si(OPO)_3]^+$, which range from 86.62° to 87.26°.[19] The O_2Si chelate ring and the OPO ligands form fold angles of 9.67(5)° and 11.47(3)° in **4**, 12.39(8)° and 12.68(10)° in **5**, and 7.79(5)° and 9.32(3)° in **6** with the pyridine rings bending toward the alkyl group.[24] The Si—O bond lengths are more similar to each other compared with those in **1**-**3** likely due to opposing disordered OPO ligands having mutually similar *trans* influences.

The preference for **4-6** to adopt pentacoordinate ion-paired structures over their neutral hexacoordinate forms appears to be a result of a greater degree of stabilizing C—H···Cl intermolecular hydrogen-bonding contacts in their structures compared with **1-3** (Figure 8). In all three cationic structures, there are three C—H···Cl intermolecular contacts of ~2.5 Å each whereas in the neutral structures fewer or longer interactions are present (Table 3).[25] It is not clear whether these interactions are the cause or the effect of chloride ion dissociation: Multiple H-bonding interactions may weaken the Si—Cl bond to form the cation, or greater accessibility for H-bonding interactions results from a sterically unencumbered chloride ion. Studies by Brendler *et al*. show that a single C—H···Cl interaction of 2.94 Å can impart measurable stability to a crystal lattice.[26]

An additional explanation that was considered for the difference in the structures of **1**-**3** and **4**-**6** was that they perhaps represented different tautomeric forms of each other, similar to behavior reported in a hydrazide-based complex,[8b] but in the present case resulting from the partial or complete loss of π-electron delocalization in one or both OPO ligands upon coordination of chloride. Shortening of the C1-N1/C6-N2 and C3-C4/C8-C9 bonds and lengthening of the C2-C3/C7-C8 and C4-C5/C9-C10 bonds is expected in moving from a localized to delocalized π-system.[27] By comparison with two known monodentate OPO complexes, which should have effectively no delocalization occurring, the largest difference between chelated and unchelated complexes was found in the C—N bond length. Specifically, the C—N bond lengths in **1**-**6** [range = 1.346(2)–1.3567(13) Å] are significantly shorter than those in $Me_3Si(\kappa^1\text{-OPO})$ [1.398(2) Å] and $^tBu_2Si(\kappa^1\text{-OPO})(\kappa^2\text{-OPO})$ [1.3994(19) Å],[17] pointing to π-electron delocalization occurring in **1**-**6**. However, a comparison between neutral **1**-**3** and cationic complexes **4**-**6**, which have different chelate strengths indicated by their Si—O bond lengths, did not reveal significant differences in their C—N bond lengths and thus does not provide evidence for tautomeric character. An ionic no bond resonance form shown in Figure 1 may be more representative of the bonding.[28] For a better understanding of the effect of π-electron delocalization on chelate strength and charge distribution in these molecules, computational studies are needed.

Considering electronics and sterics, it is perhaps surprising that the benzyl derivative **3** does not adopt a similar cationic structure as **4**-**6** which also possess alkyl ligands. One possible explanation is that a weak intramolecular π-π interaction exists between the benzyl ligand and an OPO ligand [$d_{C6\text{-}C12}$ = 3.0356(13) Å and $d_{N2\text{-}C17}$ = 3.1856(14) Å] which may contribute to the stabilization of **3** in its neutral hexacoordinate form. By comparison, the fluoride derivative, $BnSi(OPO)_2F$ (**9**) (vide infra), stabilized in its hexacoordinate form by the strong Si—F bond, exhibits weaker such interactions [$d_{C6\text{-}C12}$ = 3.4163(33) Å and $d_{N2\text{-}C17}$ = 3.5392(32) Å]. However, in **3** and **9**, the wide Si1-C11-C12 angles [116.28(7)° and 113.84(17)°, respectively][29] and the angles between the N2/C6-C10 and the C12-C17 ring planes [24.90(5)° and 23.89(8)°, respectively] seem to suggest that π overlap may be minimal and therefore that the hexacoordinate geometry of **3** may be due primarily to the benzyl group exerting an electronic effect more similar to the aryls. Comparable electronic effects have been observed in hydrazide organosilicon complexes where replacement of methyl with benzyl, and of benzyl with phenyl

ancillary ligands resulted in an increase in the barrier to dissociation of chloride by 1-2 kcal/mol.[8c] In summary, it generally follows that more electron-withdrawing groups (phenyl and *p*-tolyl) result in a stronger Si—Cl interaction than with electron-donating groups (methyl, *t*-butyl, thexyl) in line with expected inductive effects.

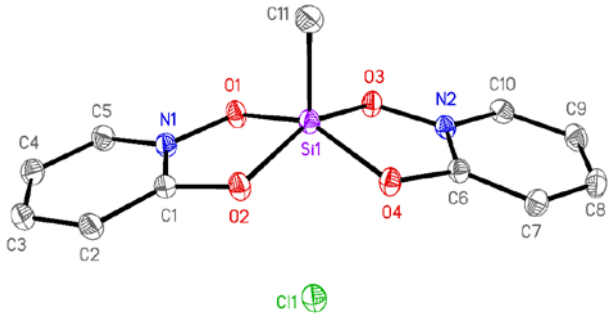

Figure 5. Thermal ellipsoid plot of **4** at the 50% probability level with hydrogen atoms omitted.

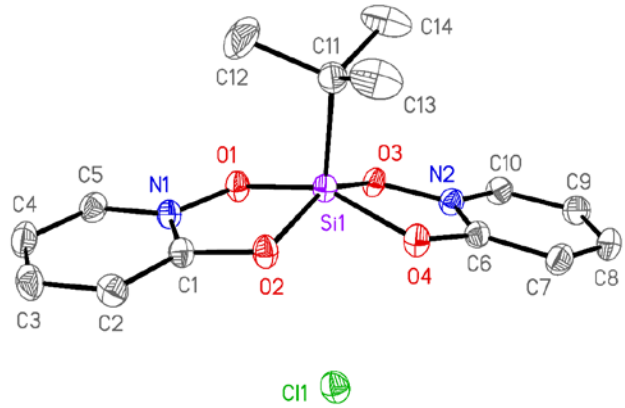

Figure 6. Thermal ellipsoid plot of **5** at the 50% probability level with hydrogen atoms omitted.

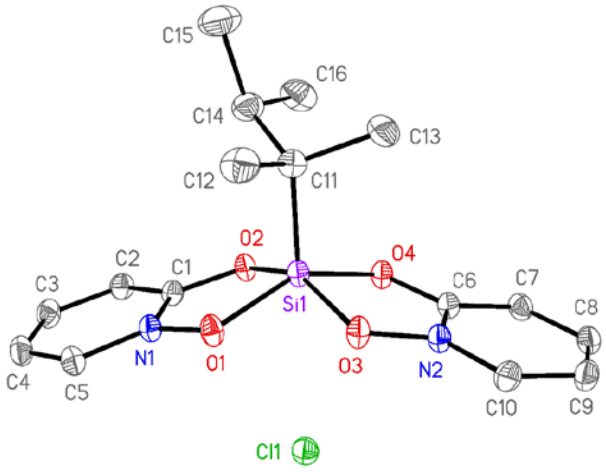

Figure 7. Thermal ellipsoid plot of **6** at the 50% probability level with hydrogen atoms omitted.

Table 2. Selected Bond Distances (Å) and Angles (°) for **4**, **5**, and **6**. None of the C-N, N-O, and C-O bond lengths can be represented accurately due to C/N site disorder.

	4	**5**	**6**
Si1-C11	1.8484(14)	1.882(2)	1.8978(13)
Si1-Cl1	3.5007(5)	3.5055(7)	3.4415(6)
Si1-O1	1.7592(10)	1.7642(11)	1.7663(9)
Si1-O2	1.7524(9)	1.7480(12)	1.7599(9)
Si1-O3	1.7489(9)	1.7573(11)	1.7460(9)
Si1-O4	1.7592(9)	1.7595(12)	1.7650(9)
O1-Si1-O2	87.39(4)	87.39(5)	86.81(4)
O3-Si1-O4	87.52(4)	87.13(5)	87.47(4)
O1-Si1-O3	148.08(5)	151.36(6)	147.24(5)
O2-Si1-O4	152.39(5)	148.01(6)	151.55(4)
C11-Si1-Cl1	176.75(5)	171.0(1)[a]	176.92(4)
O2-Si1-O3	86.00(4)	86.41(5)	85.98(4)
O1-Si1-O4	84.05(4)	83.48(5)	83.87(4)
O1-Si1-C11	106.75(6)	106.18(10)	106.08(5)
O2-Si1-C11	103.52(5)	104.87(10)	105.47(5)
O3-Si1-C11	105.16(6)	102.43(10)	106.64(5)
O4-Si1-C11	104.08(5)	107.11(10)	102.93(5)

[a] The *t*-butyl group is modeled as disordered over two positions (0.86:0.14). Only the angle for the major contributor is given.

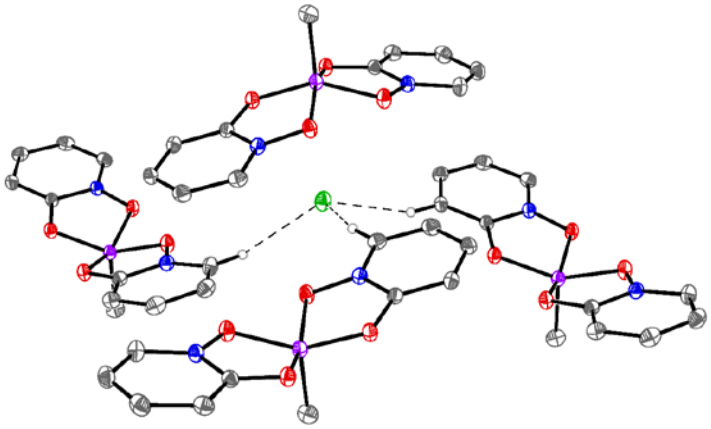

Figure 8. Three weak C—H···Cl intermolecular contacts in **4**. Contact distances and angles are given in Table 3.

Table 3. C—H···Cl intermolecular contact distances and angles in **1**-**6**.

	$d_{H\cdots Cl}$ (Å)	$\angle_{C\text{-}H\cdots Cl}$ (°)		$d_{H\cdots Cl}$ (Å)	$\angle_{C\text{-}H\cdots Cl}$ (°)
1	2.71	138.6	**4**	2.50	159.3
	2.74	169.2		2.50	158.0
	2.83	143.2		2.51	154.3
				2.90	129.0
2	2.67	170.6			
	2.82	149.0	**5**	2.49	151.5
	2.82	136.2		2.53	151.6
	2.87	152.0		2.57	162.7
3	2.67	159.3	**6**	2.55	150.3
	2.70	177.9		2.55	163.6
				2.59	149.1
				2.96	127.0
				2.97	127.0

Solution-state structures. The ^{29}Si NMR resonances of **1-5**, observed at −145.6, −145.0, −139.9, −134.0, and −133.0 ppm, respectively, all fall in the region typical of hexacoordinate silicon complexes and were virtually invariable with increased temperature.[30] The resonances for **1-3** are therefore consistent with expectations from their solid-state structures, but those of **4** and **5** differ substantially from the generally expected region for pentacoordinate complexes.[31] Among all complexes **1-6**, the positions of the five ^{13}C NMR OPO ligand resonances are virtually superimposable, with their chemical shifts deviating not more than 1.3 ppm between complexes. Each complex displays two isomers evidenced in their ^{13}C NMR spectra by the splitting of one or two carbon resonances of the OPO ligands into two closely-spaced peaks.[32] These observations and further studies described below support that all of these complexes have similar solution structures with *trans*-OPO bischelate arrangements.

The iodo and triflato derivatives, (*p*-tolyl)Si(OPO)$_2$I (**7**) and (*p*-tolyl)Si(OPO)$_2$OSO$_2$CF$_3$ (**8**), were prepared to explore the replacement of the apparently coordinated chloride ion of **2** with a more weakly-coordinating anion and to examine potential differences in the NMR chemical shifts of the complexes. Reaction of (*p*-tolyl)SiCl$_3$ with 2 equiv. of Me$_3$Si(OPO) and 1 equiv. of Me$_3$SiI or Me$_3$SiOSO$_2$CF$_3$ afforded complexes **7** and **8**, respectively, in quantitative yields (eq 2).[33,34] In DMSO-d_6, both **7** and **8** exhibited ^{1}H, ^{13}C, and ^{29}Si NMR spectra *identical* to those of **2** and therefore strongly supports that all three complexes exist as separated ion pairs in solution. The connectivity of **8** (Figure 9) was established by X-ray diffraction analysis, which revealed an SP geometry with *trans*-OPO ligands and a weakly interacting triflate ion in a regular position off of the vacant coordination site, with the shortest Si$\cdots$OSO$_2$CF$_3$ distance of

3.237(2) Å. A comparison of the X-ray structures of **2** and **8** as well as by structural analogy with **4-6** support that, in general, the *trans*-OPO SP configuration is favored when the complex becomes cationic.

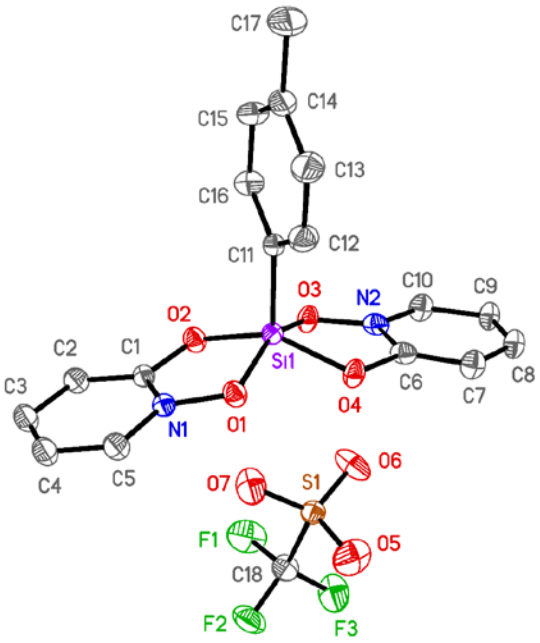

Figure 9. Thermal ellipsoid plot of **8** at the 50% probability level with hydrogen atoms omitted.

With separated ion pairs established in solution for the chloride, iodide, and triflate complexes of $[(p\text{-tolyl})Si(OPO)_2]^+$ and by ^{13}C NMR spectral analogy with all other chloride derivatives, it seemed reasonable that the pentacoordinate complexes, exhibiting high field ^{29}Si NMR resonances, were in fact, hexacoordinate DMSO adducts. The possibility of DMSO adduct formation was examined by comparing the ^1H NMR spectrum of **4** in $CDCl_3$ with spectra of solutions containing incremental additions of protio DMSO (Figure 10).[35] With the

incremental addition of four equivalents of DMSO, the $SiCH_3$ peak of **4** broadens and shifts gradually upfield by 0.35 ppm. The addition of the first equivalent of DMSO resulted in its greatest downfield shift (Δ = 0.21 ppm) from its native position and, as a result of an increase in the weighted average of free vs. coordinated DMSO, gradually shifted back toward its native position as its concentration was increased.[36] The shielding of the $SiCH_3$ proton resonance, the deshielding of the DMSO proton resonance, and that the $SiCH_3$ proton resonance is shifted to a greater extent than the OPO ligand resonances due to its proximity to the site of interaction support the formation of a DMSO adduct in solution.[37] There are very limited reports of other spectroscopically-characterized DMSO adducts of hypercoordinate silicon with one well-documented example reported by Wagler et al. of a cationic salen-type DMSO adduct complex in equilibrium with its non-adduct.[21a] The observation of a single DMSO peak at all concentrations and a gradual shift of the resonances with increasing concentration indicates a similar solvation equilibrium, but unlike in the salen complex where the authors proposed the absence of DMSO-anion exchange, we have garnered indirect evidence for DMSO-anion exchange by the isolation of a crystal of **4**·2$CDCl_3$ from a saturated $CDCl_3$ solution containing DMSO, and the lack of observation of the expected ^{13}C NMR resonance of the CF_3 group in complex **8**, presumably broadened due to fluxional exchange. The indications for DMSO adduct formation therefore explain the observed high field ^{29}Si NMR resonances typical of hexacoordinate complexes. The related cationic complexes, $[RSi(tropolonato)_2]^+Cl^-$ [R = CH_3, $(CH_2)_4CH_3$, $CH{=}CH_2$, C_6H_5] and $[PhSi(PhC(O)CHC(O)Ph)_2]^+HCl_2^-$ purported to be pentacoordinate, also exhibit high-field ^{29}Si NMR chemical shifts ranging from −127.1 ppm to −175.8 ppm in DMSO-d_6 and are therefore likely to be DMSO adducts as well.[38] Furthermore, other cationic complexes with SiCO_4 cores, specifically [RSi(*N*,*N*-dimethylhydroxyacetamide)$_2$]$^+$ {R = Ph, ^{t}Bu, $BrCH_2$}, exhibit ^{29}Si NMR resonances in $CDCl_3$ or CD_3CN in the range of −59.5 ppm to −77.2 ppm, consistent with pentacoordination.[15]

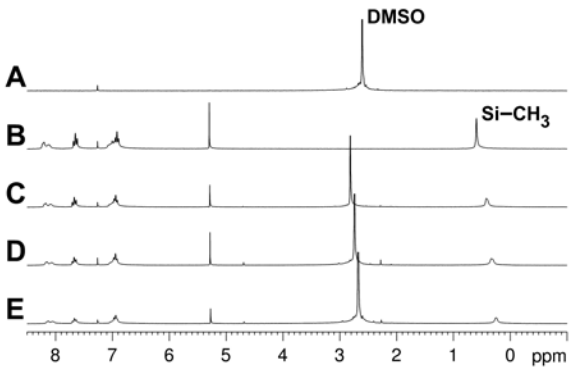

Figure 10. ^{1}H NMR spectra of DMSO only in $CDCl_3$ (**A**) and of **4**·CH_2Cl_2 in $CDCl_3$ with added DMSO (**B** = 0 equiv.; **C** = 1 equiv.; **D** = 2 equiv.; **E** = 4 equiv.).

Unfortunately, attempts to crystallize a DMSO adduct were unsuccessful. Crystals analyzing as **4**·2$CDCl_3$ deposited from a $CDCl_3$ solution of **4** containing DMSO, and crystals of **6** were obtained by crystallization from neat DMSO-d_6, presumably due to greater lattice energies of the non-adducts. Recrystallization attempts of **7** from DMSO-containing solvent systems all precipitated as oils.

As points of contrast, the synthesis of related non-adduct complexes was pursued by replacing chloride with the more strongly coordinating fluoride ion. $BnSi(OPO)_2F$ (**9**) and $MeSi(OPO)_2F$ (**10**) were prepared in quantitative yield by reaction of 1 equiv. Me_3SnF with **3** and **4**, respectively (eq 3). In DMSO-d_6, the temperature-independent ^{29}Si NMR resonances for **9** and **10** appear at −141.3 ppm and −135.2 ppm, respectively, supporting their hexacoordinate geometries. Evidence for fluoride coordination in both complexes is given by coupling with fluorine [$^{1}J_{SiF}$ (~250 Hz) and $^{2}J_{CF}$ (~45 Hz)] which was maintained at high temperature.[39] The NMR spectra of **9** and **10** at room temperature are more complex than those of **3** and **4**, and display more than two closely-spaced peaks of some of the carbon resonances of the OPO ligands. With this evidence of more than two isomers, a *cis*-OPO ligand arrangement is indicated for which there are four possible isomers.

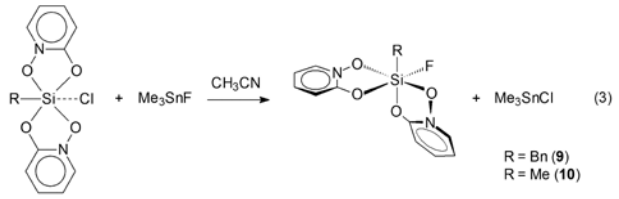

The X-ray crystal structures of the fluoride derivatives **9** and **10** (Figures 11 and 12) show distorted octahedral geometries with *cis*-OPO ligands. Selected bond distances and angles for **9** and **10** are given in Table 1. Relative to their respective chloride analogs **3** and **4**, the structure of **9** is similar, but the structure of **10** differs not only by the coordination of the halide, but also a change in the conformation of the OPO ligands from *trans* to *cis*. These observations are consistent with the solution structures described above. As with the comparison between the solid-state structures of **2** and **8**, a comparison of structures **4** and **10** also supports the conclusion that a *cis*-OPO conformation of the complexes is favored with more strongly coordinating anions and that a *trans*-OPO conformation is favored with dissociated or weakly-coordinating anions.

The Si—O distances are all slightly longer and the O_2Si bite angles are smaller (Δ=1.36-1.78°) in **9** compared to those of **3**. Similarly, in **10**, the Si—O bond distances are longer and the O_2Si bite angles are smaller (Δ=3.0-3.6°) compared to those of its cationic chloride derivative **4**. These structural features reflect an overall weaker OPO chelate interaction in the fluoride derivatives. Despite the greater electron-withdrawing ability of F vs. Cl, the reduced electrophilicity of Si in these complexes is attributed to the greater Si—F covalent bonding contribution, as well as the increased electrophilicity of Si in **4** vs. **10** due to ionization. Lengthening of Si—O bonds was also observed in 2-acylpyrole complexes upon the exchange of chlorine with fluorine,[10] but less so in oxinate complexes.[9b]

Both **9** and **10** exhibited ligand C/N site disorder in their structures and like **1**, **2**, and **3**, the statistical disorder ratios indicate the major isomer in each to have an O(N)-*trans*-O(N) arrangement (see Experimental Section). The presence of multiple isomers is consistent with more than two isomers observed in their solution NMR spectra. VT-NMR experiments described below show these isomers to be in equilibrium.

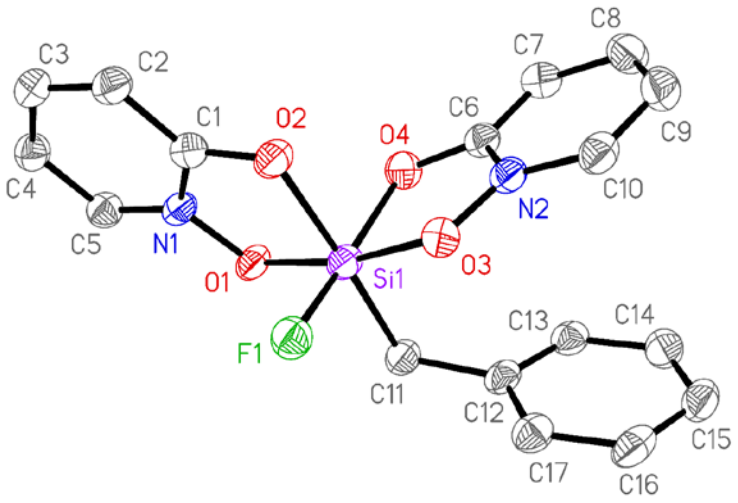

Figure 11. Thermal ellipsoid plot of **9** at the 50% probability level with hydrogen atoms omitted. Selected bond distances and angles are given in Table 1.

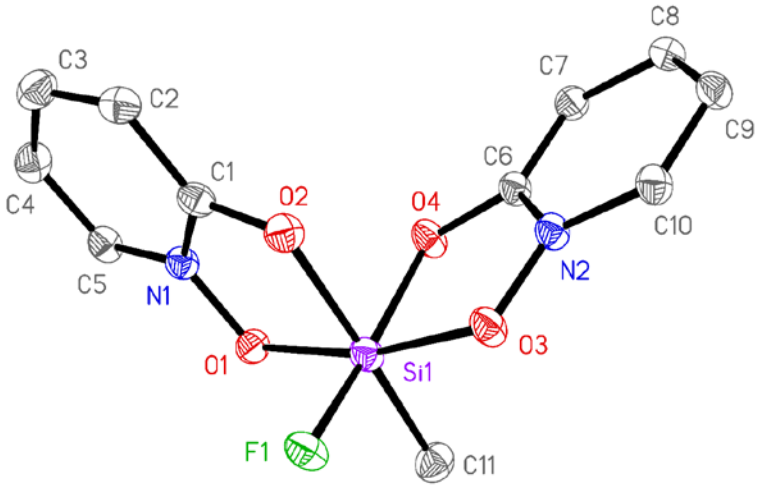

Figure 12. Thermal ellipsoid plot of **10** at the 50% probability level with hydrogen atoms omitted. Selected bond distances and angles are given in Table 1.

Variable-Temperature NMR studies. The ^{1}H NMR spectrum of **4** at room temperature indicates the presence of two isomers in approximately 1:1 ratio which is evidenced by two closely-spaced peaks for the methyl protons and two sets of well-defined doublets at 8.7 ppm representing CH protons adjacent to nitrogen (Figure 13). These isomers are assigned on several bases to the two possible isomers of $[MeSi(OPO)_2(DMSO)]^+$ having *trans*-OPO ligands: (1) The

X-ray structures of **1**-**6** and **8**-**10** show that the metal core consistently prefers *trans*-OPO ligands when anions are dissociated/weakly coordinated and *cis*-OPO ligands when anions are coordinated more strongly; (2) Separated ion pairs are present and DMSO coordinates weakly as described above; (3) A core structure having *cis*-OPO ligands would allow for four possible isomers of similar energies on the basis of ligand C/N site disorder observed in the X-ray structures of **1**-**3** of which would be expected to produce more complex NMR spectra similar to those of **9** and **10**.

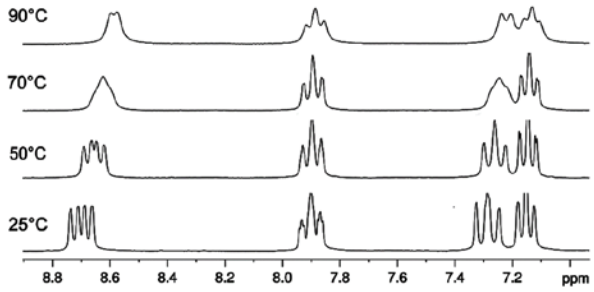

Figure 13. Partial variable-temperature ^{1}H NMR spectra of **4** in DMSO-d_6.

VT-NMR studies of **1**-**6** in DMSO-d_6 all show evidence of the interconversion between the O(N)-*trans*-O(N) and O(N)-*trans*-O(C) isomers (eq 4). In the spectrum of **4**, as the temperature is increased, the two doublets at 8.7 ppm coalesce at ~70 °C and resolve to one broad doublet at ~90 °C, the multiplet at 7.3 ppm resolves into a doublet, and the double resonances of the Si-CH_3 peak (not shown) resolve into a singlet as the two isomers become magnetically equivalent. In the ^{13}C NMR spectrum of **4** at 25 °C, the two OPO ligand resonances (δ = 115 and δ = 140) each displaying two closely-spaced resonances for the two isomers also coalesce to single peaks at 70 °C. Similar reversible behavior was observed in the ^{13}C NMR spectra of all of the other chloride complexes and suggests a common process for all. Taken as an AB site exchange, the activation energies ($\Delta G^{\ddagger}$) were calculated using the ^{13}C NMR data and the formulae: $k = 2\pi(\Delta\nu)/\sqrt{2}$ and $\Delta G^{\ddagger} = -RT(\ln k - \ln (k_b T/h))$. Complexes **1**-**6** were all found to interconvert with remarkably similar activation energies (18-19 kcal/mol) despite differences of the R substituent (see the Supporting Information).[40] Additionally, the *p*-tolyl chloride **2** and triflate **8** derivatives were found to have identical rates of exchange and

coalescence temperatures which further supports ion pair separation in solution and dynamic exchange of the same cationic complex.

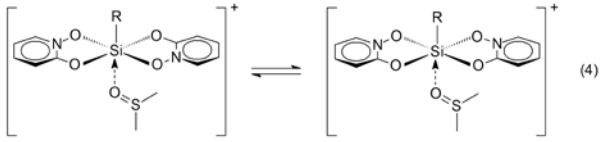

(4)

Considering the evidence for lability of DMSO, and that dissociation of DMSO should be favored at higher temperatures,[21a] a Berry twist mechanism involving a pentacoordinate TBP_{eq} intermediate is proposed (Figure 14). A TBP_{ax} intermediate would be disfavored due to significant chelate ring strain resulting upon spanning two equatorial sites as well as a greater number of 90° steric interactions resulting between the R group and the OPO ligands. Ab initio calculations reported for the two pathways in the related model catecholate complex ion, $[HSi(cat)_2]^-$, suggest the barrier to isomerization is 14.5 kcal·mol^{-1} higher through its TBP_{ax} intermediate.[41] The possibility of an isomerization equilibrium between *trans*-OPO and *cis*-OPO bischelates also occurring cannot be ruled out, although there is no spectroscopic evidence for this. Stereoisomerization mechanisms in hypercoordinate silicon complexes have been studied extensively.[42]

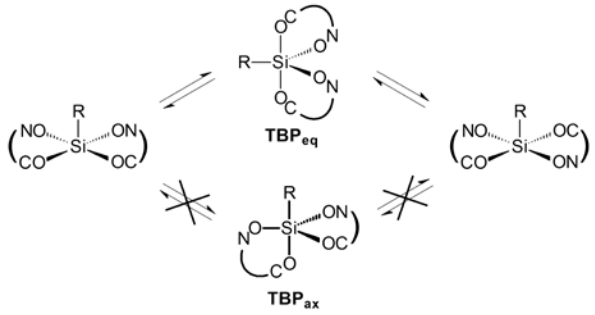

Figure 14. Proposed mechanism for the interconversion of O(N)-*trans*-O(N) and O(N)-*trans*-O(C) isomers in $[RSi(OPO)_2]^+$ complexes.

^{13}C VT-NMR studies of both of the fluoride derivatives **9** and **10** in DMSO-d_6 indicate equilibria between the multiple observed isomers. Broadened and overlapping OPO ligand resonances are present at room temperature and coalesce upon heating to ~80 °C for **9** and to ~50

°C for **10** (See the Supporting Information). In **10**, the ^{1}H NMR methyl resonance remains a doublet up to 80 °C and indicates that the Si—F bond remains intact. Complexes **9** and **10** both exhibited ^{29}Si NMR downfield shifts of 0.01 ppm/°C upon increasing the temperature from 25 to 60 °C, and although small, this rate of shift is not inconsistent with dative Si←OC bond dissociation occurring as has been established to occur in the related neutral $R_2Si(OPO)_2$ complexes.[17] In contrast, however, the OPO ^{13}C NMR resonances of **9** and **10** did not shift in the directions indicative of Si←OC bond dissociation, and this may suggest a non-dissociative ligand exchange mechanism, as determined for related monoorgano bis(hydrazide) halide complexes.[22a,39a]

Conclusion. In the solid state, the neutral structures of **1-3** and the cationic structures of **4-6** are consistent with more strongly electron-donating R groups favoring chloride dissociation. Crystal packing arrangements that allow for multiple weak C—H···Cl hydrogen-bonding interactions also facilitate chloride dissociation. Independent of the carbon-based substituent, upon anion dissociation, a change in conformation from *cis*-OPO to effectively *trans*-OPO bischelates occurs in both the solid and solution states. Activation barriers for the dynamic isomerization of the DMSO-adduct complexes of **1-6** are also largely unaffected by the electronic and steric character of the R substituent.

Acknowledgments. The authors thank St. John Fisher College and the University of Rochester Chemistry Department for support.

Experimental Section. All manipulations were performed inside a N_2-filled Vacuum Atmospheres glovebox. Acetonitrile, dichloromethane, and chloroform were dried and vacuum-distilled from activated 4Å molecular sieves. Diethyl ether and THF were distilled from purple solutions of benzophenone ketyl and stored over 4Å molecular sieves. Toluene, DMSO, and DMSO-d_6 were passed through activated alumina prior to use. Silyl chlorides, $Me_3SiOSO_2CF_3$, Me_3SiI, and Me_3SnF were purchased from Gelest, Inc. and used as received. $Me_3Si(OPO)$ was prepared as described previously.[17] ^{1}H, ^{13}C, and ^{29}Si NMR spectra were recorded using a Bruker DPX250 NMR spectrometer (^{1}H, 250.1 MHz; ^{13}C, 62.9 MHz; ^{29}Si, 49.7 MHz) with ^{29}Si NMR spectra recorded at a minimum resolution of 0.36 Hz. ^{29}Si NMR chemical shifts were referenced using pure TMS external capillary standards. All samples for elemental analysis were obtained

directly after workup of the synthesis and were performed at the CENTC Elemental Analysis Facility at the University of Rochester.

Single crystal X-ray crystallography. Crystals were placed onto the tips of glass optical fibers and mounted on a Bruker SMART platform diffractometer equipped with an APEX II CCD area detector for data collection.[43] For each crystal a preliminary set of cell constants and an orientation matrix were calculated from reflections harvested from three orthogonal wedges of reciprocal space. Full data collections were carried out using MoKα radiation (0.71073 Å, graphite monochromator) with frame times ranging from 10 to 120 seconds and at detector distances of approximately four cm. Randomly oriented regions of reciprocal space were surveyed: four to six major sections of frames were collected with 0.50º steps in ω at four to six different φ settings and a detector position of -38º in 2θ. The intensity data were corrected for absorption.[44] Final cell constants were calculated from the xyz centroids of about 4000 strong reflections from the actual data collections after integration.[45]

Structures were solved using SIR97[46] or SHELXT-2014/5[47] and refined using SHELXL-2014/7.[48] Space groups were determined based on systematic absences, intensity statistics, or both. Direct-methods solutions were calculated which provided most non-hydrogen atoms from the E-map. Full-matrix least squares / difference Fourier cycles were performed which located the remaining non-hydrogen atoms. All non-hydrogen atoms were refined with anisotropic displacement parameters. All hydrogen atoms were placed in ideal positions and refined as riding atoms with relative isotropic displacement parameters. Full matrix least squares refinements on F^2 were run to convergence.

The crystal of **1** was a non-merohedral twin. Application of twin law [-1 0 0 / 0 -1 0 / 0.751 0 1], a 180 degree rotation about reciprocal lattice [001], improved the *R*1 residual for strong data from 0.151 to 0.046. The crystal of **9** was a pseudo-merohedral twin, for which the monoclinic unit cell could transform to side-centered orthorhombic. Application of twin law [1 0 0 / 0 -1 0 / -1 0 -1], a 180 degree rotation around direct lattice [100], reduced the *R*1 residual for strong data from 0.112 to 0.055.

Both of the bidentate ligands in **1** are modeled as disordered with the planar flips of themselves (0.78:0.22 and 0.65:0.35, for ligands containing O1/O2 and O3/O4, respectively). The disorder in each bidentate ligand was modeled by refining the sites of the nitrogen and

oxygen-coordinated carbon atoms as a mixture of the two atom types. In each site, the two atom types were constrained to have equivalent positional and anisotropic displacement parameters. For each ligand the sum of the occupancies of the two atom types over those two sites was constrained to be exactly one of each atom type. Analogous disorders occur for both chelating ligands in **2** (0.72:28 and 0.70:0.30), in **3** (0.58:42 and 0.73:27), in **4** (0.69:0.31 and 0.54:0.46), in **5** (0.53:0.47 and 0.65:0.35), in **6** (0.63:0.37 and 0.58:0.42), in **9** (0.85:0.15 and 0.84:0.16), and in **10** (0.88:0.12 and 0.65:0.35).

2 cocrystallized with one molecule of chloroform, which was modeled as disordered over two positions (0.90:0.10). One molecule of dichloromethane cocrystallized with **4** and the *tert*-butyl group of **5** is modeled as disordered over two positions (0.86:0.14). In all structures except **8**, all species are found in general positions. In **8** the asymmetric unit contains one half of a silicon complex cation, one half of a triflate anion, and one half of a cocrystallized THF solvent molecule, all located on crystallographic mirror planes, and with one mirror essentially bisecting the chelating ligands. All species were modeled as disordered over their respective mirror planes (0.50:0.50). The triflate anion and THF solvent molecule are each modeled as disordered over an additional position (0.90:0.10 and 0.84:0.16, respectively). Additionally, all four Si—O bond lengths were restrained to be similar; however, it is known that these distances can vary with the orientation of the chelating ligand. Crystallographic data have been deposited with the Cambridge Crystallographic Data Centre (CCDC).

$PhSi(OPO)_2Cl{\cdot}xCHCl_3$ (1). A solution of $Me_3Si(OPO)$ (0.202 g, 1.10 mmol) in 10 mL of $CHCl_3$ was added to a solution of $PhSiCl_3$ (0.116 g, d = 1.324 g/mL, 0.548 mmol) in 5 mL of $CHCl_3$ and allowed to stand undisturbed. Precipitation of colorless X-ray quality crystals of $PhSi(OPO)_2Cl{\cdot}CHCl_3$ occurred after 1 day which were isolated by filtration. Drying under prolonged vacuum at 130 °C afforded 0.137 g (69.0%) of $PhSi(OPO)_2Cl$ contaminated with a small amount of $CHCl_3$. ^{1}H NMR (DMSO-d_6): δ 7.20 (br m, 6H), 7.40 (br d, 1H), 7.59 (br m, 2H), 7.95 (br t, 2H, C*H*CHCO), 8.78 (br m, 2H, CHN). ^{13}C NMR (DMSO-d_6): δ 112.9 (*C*HCHN), 115.9 (*C*HCO), 127.4 (Ar), 127.5 (Ar), 133.9 (CHN), 134.2 (Ar), 140.5 (*C*HCHCO), 147.4 (SiC), 154.5 (CO). ^{29}Si NMR (DMSO-d_6): δ –145.6. Quantitative ^{1}H NMR data was consistent with ~0.04 mol $CHCl_3$/mol Si. Anal. Calcd for $C_{16}H_{13}ClN_2O_4Si{\bullet}0.04CHCl_3$: C, 52.69; H, 3.60; N, 7.66. Found: C, 52.75; H, 3.52; N, 7.60.

(*p*-tolyl)Si(OPO)$_2$Cl (2). A solution of $Me_3Si(OPO)$ (0.201 g, 1.10 mmol) in 10 mL of $CHCl_3$ was added to a solution of (*p*-tolyl)$SiCl_3$ (0.124 g, d = 1.273 g/mL, 0.549 mmol) in 5 mL of $CHCl_3$ upon which a precipitate formed within a few minutes. Vacuum filtration and drying under vacuum afforded 0.206 g (90.7%) of white powder. X-ray quality crystals of (*p*-tolyl)Si(OPO)$_2$Cl·$CHCl_3$ were obtained from an undisturbed mixture of the same reaction at 25% of the original concentration. ^{1}H NMR (DMSO-d_6): δ 2.23 (s, 3H, CH_3), 7.02 (br d, 2H, Ar), 7.20 (br t, 2H, C*H*CHN), 7.35 (br d, 2H, CHCO), 7.47 (br d, 2H, Ar), 7.94 (br t, 2H, C*H*CHO), 8.74 (br m, 2H, CHN). ^{13}C NMR (DMSO-d_6): δ 20.9 (CH_3), 112.4 (*C*HCHN), 115.4 (*C*HCO), 127.6 (Ar), 133.1 (CHN), 133.8 (Ar), 135.9 (Ar), 140.0 (*C*HCHCO), 154.0 (CO). ^{29}Si NMR (DMSO-d_6): δ –145.0. Anal. Calcd for $C_{17}H_{15}ClN_2O_4Si$: C, 54.47; H, 4.03; N, 7.47. Found: C, 54.13; H, 3.95; N, 7.50.

BnSi(OPO)$_2$Cl (3). A solution of $Me_3Si(OPO)$ (0.200 g, 1.10 mmol) in 10 mL of $CHCl_3$ was added to a solution of $BnSiCl_3$ (0.123 g, d = 1.288 g/mL, 0.546 mmol) in 5 mL of $CHCl_3$ upon which a precipitate gradually formed over a period of 1 day. Vacuum filtration and drying under vacuum afforded 0.131 g (64.2%) of white powder. X-ray quality crystals were obtained from the undisturbed reaction mixture of the same synthesis in CH_3CN. ^{1}H NMR (DMSO-d_6): δ 2.20 (s, 2H, CH_2), 6.90 (br m, 5H), 7.10 (br t, 2H, C*H*CHN), 7.20 (br m, 2H, CHCO), 7.86 (br t, 2H, C*H*CHCO), 8.58 (br m, 2H, CHN). ^{13}C NMR (DMSO-d_6): δ 34.2 (CH_2), 112.6 (*C*HCHN), 115.6 (*C*HCO), 123.4 (Ar), 127.7 (Ar), 128.7 (Ar), 133.3 (CHN), 140.2 (*C*HCHCO), 143.9 (*C*CH_2), 154.4 (CO). ^{29}Si NMR (DMSO-d_6): δ –139.91, –139.86. Anal. Calcd for $C_{17}H_{15}ClN_2O_4Si$: C, 54.47; H, 4.03; N, 7.47. Found: C, 54.21; H, 3.98; N, 7.33.

MeSi(OPO)$_2$Cl (4). A solution of $Me_3Si(OPO)$ (0.201 g, 1.10 mmol) in 10 mL of CH_2Cl_2 was added to a solution of $MeSiCl_3$ (0.082 g, d = 1.275 g/mL, 0.58 mmol) in 5 mL of CH_2Cl_2 and allowed to stand undisturbed. Precipitation of colorless X-ray quality crystals of MeSi(OPO)$_2$Cl·CH_2Cl_2 occurred after ~1 day which were isolated by filtration. Drying under vacuum at 130 °C afforded 0.105 g (64.5%) of MeSi(OPO)$_2$Cl. ^{1}H NMR (DMSO-d_6): δ 0.13 (s, 3H, SiMe), 7.15 (br t, 2H, C*H*CHN), 7.29 (br m, 2H, CHCO), 7.90 (br m, 2H, C*H*CHCO), 8.70 (two br d, 2H, CHN). ^{13}C NMR (DMSO-d_6): δ 7.9 (SiMe), 112.7 (*C*HCHN), 115.5 (*C*HCO),

133.5 (CHN), 140.2 (*C*HCHCO), 154.5 (CO). ^{29}Si NMR (DMSO-d_6): δ −134.0. Anal. Calcd for $C_{11}H_{11}ClN_2O_4Si$: C, 44.22; H, 3.71; N, 9.38. Found: C, 44.28; H, 3.67; N, 9.26.

^{t}BuSi(OPO)$_2$Cl·xCHCl$_3$ (5). A solution of $Me_3Si(OPO)$ (0.204 g, 1.11 mmol) in 10 mL of $CHCl_3$ was added to a solution of ^{t}BuSiCl$_3$ (0.107 g, d = 1.161 g/mL, 0.559 mmol) in 5 mL of $CHCl_3$ upon which a precipitate formed within a few minutes. Vacuum filtration and prolonged drying under vacuum afforded 0.183 g (76.1%) of white powder analyzing as ^{t}BuSi(OPO)$_2$Cl·0.75CHCl$_3$. ^{1}H NMR (DMSO-d_6): δ 0.88 (s, 9H, ^{t}Bu), 7.15 (br t, 2H, C*H*CHN), 7.30 (br m, 2H, CHCO), 7.91 (br m, 2H, C*H*CHCO), 8.41 (s, 0.75 H, $CHCl_3$), 8.71 (br m, 2H, CHN). ^{13}C NMR (DMSO-d_6): δ 27.5 (*C*(CH$_3$)$_3$), 31.6 (C(*C*H$_3$)$_3$), 79.3 ($CHCl_3$), 112.7 (*C*HCHN), 115.7 (*C*HCO), 133.5 (CHN), 140.2 (*C*HCHCO), 154.6 (CO). ^{29}Si NMR (DMSO-d_6): δ −133.06, −132.96. Quantitative ^{1}H NMR data was consistent with ~0.75 mol $CHCl_3$/mol Si. Anal. Calcd for $C_{14}H_{17}ClN_2O_4Si$•0.75$CHCl_3$: C, 41.16; H, 4.16; N, 6.51. Found: C, 40.84; H, 3.96; N, 6.30. X-ray quality crystals of ^{t}BuSi(OPO)$_2$Cl were obtained from an undisturbed reaction mixture of the above synthesis in acetonitrile.

(thexyl)Si(OPO)$_2$Cl (6). A solution of $Me_3Si(OPO)$ (0.1953 g, 1.066 mmol) in 10 mL of CH_3CN was added to a solution of (thexyl)$SiCl_3$ (100. μL, d = 1.17 g/mL, 0.533 mmol) in 4 mL of CH_3CN upon which a precipitate formed within a few minutes. Vacuum filtration and prolonged drying under vacuum afforded 0.115 g (58.5%) of white powder. X-ray quality crystals of (thexyl)Si(OPO)$_2$Cl precipitated from a solution of 21 mg of **6** in ~0.5 mL of DMSO-d_6. ^{1}H NMR (DMSO-d_6): δ 0.85 (m, 12H), 1.52 (m, 1H), 7.30 (br m, 2H, C*H*CHN), 7.49 (br t, 2H, CHCO), 8.05 (br m, 2H, C*H*CHCO), 8.90 (two br d, 2H, CHN). ^{13}C NMR (DMSO-d_6): δ 18.6, 18.8, 23.1, 23.6, 31.5 (br), 34.7 (br) 112.1, 112.2 (*C*HCHN), 116.1 (*C*HCO), 132.9 (CHN), 140.6, 141.3 (*C*HCHCO), 153.8 (CO). ^{29}Si NMR (DMSO-d_6): No peak found. Anal. Calcd for $C_{16}H_{21}ClN_2O_4Si$: C, 52.09; H, 5.74; N, 7.59. Found: C, 51.94; H, 5.68; N, 7.81.

(*p*-tolyl)Si(OPO)$_2$I (7). A solution of $Me_3Si(OPO)$ (0.122 g, 0.665 mmol) in ~12 mL of CH_3CN was added to a solution of (*p*-tolyl)$SiCl_3$ (0.075 g, d = 1.273 g/mL, 0.332 mmol) in ~4 mL of CH_3CN and stirred for 5 minutes. Me_3SiI (45 μL, d = 1.470 g/mL, 0.33 mmol) was added via syringe and the resulting homogenous solution was stirred for 30 min. The volatiles were

removed under vacuum and dried for several hours to yield 0.155 g (100%) of pale yellow powder. Recrystallization from CH_3CN/Et_2O by the diffusion method produced well-formed crystals, but were not suitable for X-ray analysis. The ^1H, ^{13}C, and ^{29}Si NMR spectra in DMSO-d_6 were identical to those reported for **2**. Anal. Calcd for $C_{17}H_{15}IN_2O_4Si$: C, 43.79; H, 3.24; N, 6.01. Found: C, 43.99; H, 3.18; N, 6.09.

(*p*-tolyl)Si(OPO)$_2$(OSO$_2$CF$_3$) (8). A solution of $Me_3Si(OPO)$ (0.122 g, 0.665 mmol) in ~12 mL of CH_3CN was added to a solution of (*p*-tolyl)$SiCl_3$ (0.075 g, d = 1.273 g/mL, 0.332 mmol) in ~4 mL of CH_3CN and stirred for 5 minutes. $Me_3SiOSO_2CF_3$ (60 μL, d = 1.225 g/mL, 0.33 mmol) was added via syringe and the resulting homogenous solution was stirred for 30 min. The volatiles were removed under vacuum and dried for several hours to yield 0.163 g (100%) of a white powder. Crystals of (*p*-tolyl)$Si(OPO)_2(OSO_2CF_3)$·THF used for X-ray structure analysis were obtained by recrystallization from CH_3CN/THF by the diffusion method. The ^1H, ^{13}C, and ^{29}Si NMR spectra in DMSO-d_6 were identical to those reported for **2**. The ^{13}C NMR resonance of the triflate ion could not be located, presumably broadened due to fluxional behavior. Anal. Calcd for $C_{18}H_{15}F_3N_2O_7SSi$: C, 44.26; H, 3.10; N, 5.73. Found: C, 44.10; H, 3.04; N, 5.62.

BnSi(OPO)$_2$F (9). A solution of **3** (0.0425 g, 0.113 mmol) at room temperature, prepared by boiling in ~8 mL of CH_3CN, was added to a suspension of Me_3SnF (0.0207 g, 0.113 mmol) in ~1 mL of CH_3CN. The mixture was brought to a boil until the solid dissolved, allowed to cool, and the volatiles removed under vacuum to yield 0.0404 g (99.5%) of white powder. X-ray quality crystals were obtained by recrystallization from hot DMSO-d_6/toluene (~25:75 volume ratio). Some peaks are broad in the ^1H and ^{13}C NMR spectra at room temperature and more than one isomer is indicated (see the Supporting Information). ^1H NMR (DMSO-d_6): δ 2.07 (m, 2H, CH_2), 6.86 (br m, 9H), 7.58 (br, 1H), 7.74 (t, 1H), 8.18 (m, 1H), 8.43 (t, 0.4H), 8.60 (t, 0.6H). ^{13}C NMR (DMSO-d_6): δ 32.7 ($^2J_{CF}$ = 44 Hz), 111.2-114.5, 122.1 (Ar), 126.8 (Ar), 128.1 (Ar), 132.1-132.5, 137.3, 138.2, 138.6, 145.0 (Ar), 154.4, 154.8. ^{29}Si NMR (DMSO-d_6): δ –141.3 ($^1J_{SiF}$ = 250 Hz). Anal. Calcd for $C_{17}H_{15}FN_2O_4Si$: C, 56.97; H, 4.22; N, 7.82. Found: C, 56.76; H, 4.19; N, 7.37.

MeSi(OPO)$_2$F (10). A solution of **4**·CH_2Cl_2 (0.1057 g, 0.2755 mmol) at room temperature, prepared by boiling in ~10 mL of CH_3CN, was added to a suspension of Me_3SnF (0.0504 g, 0.276 mmol) in ~2 mL of CH_3CN. The mixture was brought to a boil until the solid dissolved, allowed to cool, and the volatiles removed under vacuum to yield 0.0781 g (100%) of white powder. X-ray quality crystals were obtained by recrystallization from $CHCl_3$/Et_2O by the diffusion method. All peaks are broad in the ^{1}H and ^{13}C NMR spectra at room temperature and more than one isomer is indicated (see the Supporting Information). ^{1}H NMR (DMSO-d_6): δ –0.07 (d, J = 5.9 Hz), 6.97 (~3H), 7.19 (~1H), 7.72 (t, 2H), 8.41 (~1H), 8.53 (~3H). ^{13}C NMR (DMSO-d_6): δ 5.6 (d, $^2J_{CF}$ = 45 Hz), 111.7, 111.9, 112.5, 114.1, 132.6, 137.4, 138.4, 154.6. ^{29}Si NMR (DMSO-d_6): δ –135.2 ($^1J_{SiF}$ = 246 Hz). Anal. Calcd for $C_{11}H_{11}FN_2O_4Si$: C, 46.80; H, 3.93; N, 9.92. Found: C, 46.54; H, 3.86; N, 10.20.

Supporting Information

Crystallographic tables, CIFs, NMR spectra. This material is available free of charge via the Internet at http://pubs.acs.org.

Author Information

Corresponding Author

* E-mail: bkraft@sjfc.edu

Notes

The authors declare no competing financial interest.

---

(1) For reviews on hypercoordinate silicon complexes, see (a) Tacke, R.; Pülm, M.; Wagner, B. *Adv. Organomet. Chem.* **1999**, *44*, 221. (b) Kira, M.; Zhang, L.-C. *The Chemistry of Hypervalent Compounds*; Akiba, K.-Y., Ed.; Wiley-VCH: Weinheim, Germany, 1999; p 147. (c) Chuit, C.; Corriu, R. J. P.; Reyé, C.; Young, J. C. In *Chemistry of Hypervalent Compounds*; Akiba, K.-Y., Ed.; Wiley-VCH: New York, 1999; p 81. (d) Holmes, R. R. *Chem. Rev.* **1990**, *90*, 17. (e) Bassindale, A. R.; Glynn, S. J.; Taylor, P. G. In *The Chemistry of Organic Silicon Compounds*; Rappoport, Z.; Apeloig, Y., Eds.; Wiley: Chichester, U.K., 1998; vol. 2, part 1, p 495. (f) Kost, D.; Kalikhman, I. In *The Chemistry of Organic Silicon Compounds*; Rappoport,

Z.; Apeloig, Y., Eds.; Wiley: Chichester, U.K., 1998; vol. 2, p 1339. (g) Brook, M. A. *Silicon in Organic Organometallic and Polymer Chemistry*; Wiley: New York, 2000; p 97. (h) Holmes, R. R. *Chem. Rev*. **1996**, *96*, 927. (i) Corriu, R. J. P.; Young, J. C. In *The Chemistry of Organic Silicon Compounds*; Patai, S., Rappoport, Z., Eds.; Wiley: Chichester, U.K., 1989; vol. 1, p 1241. (j) Tacke, R.; Seiler, O. In *Silicon Chemistry: From the Atom to Extended Systems*; Jutzi, P., Schubert, U., Eds.; Wiley-VCH: Weinheim, Germany, 2003; p 324. (k) Chuit, C.; Corriu, R. J. P.; Reye, C.; Young, J. C. *Chem. Rev.* **1993**, *93*, 1371. (l) Nikolin, A. A.; Negrebetsky, V. V. *Russ. Chem. Rev.* **2014**, *83*, 848. (m) Wagler, J.; Böhme, U.; Kroke, E. *Struct. Bond.* **2014**, *155*, 29. (n) Peloquin, D. M.; Schmedake, T. A. *Coord. Chem. Rev.* **2016**, *323*, 107.

(2) For more recent contributions to the field of hypercoordinate organosilicon chemistry, see (a) González-García, G.; Álvarez, E.; Gutiérrez, J. A. *Polyhedron* **2012**, *41*, 127. (b) Weiß, J.; Sinner, K.; Baus, J. A.; Burschka, C.; Tacke, R. *Eur. J. Inorg. Chem.* **2014**, 475. (c) Voronkov, M. G.; Grebneva, E. A.; Albanov, A. I.; Zel'bst, E. A.; Trofimova, O. M.; Vasil'ev, A. D.; Chernov, N. F.; Timofeeva, E. N. *J. Organomet. Chem.* **2014**, *768*, 10. (d) Weiß, J.; Theis, B.; Baus, J. A.; Burschka, C.; Bertermann, R.; Tacke, R. *Z. Anorg. Allg. Chem.* **2014**, *640*, 300. (e) Breiding, T.; Henker, J.; Fu, C.; Xiang, Y.; Glöckner, S.; Hofmann, P.; Harms, K.; Meggers, E. *Eur. J. Inorg. Chem.* **2014**, 2924. (f) Weiss, J.; Baus, J. A.; Burschka, C.; Tacke, R. *Eur. J. Inorg. Chem.* **2014**, 2449. (g) Maguylo, C.; Chukwu, C.; Aun, M.; Monroe, T. B.; Ceccarelli, C.; Jones, D. S.; Merkert, J. W.; Donovan-Merkert, B. T.; Schmedake, T. A. *Polyhedron* **2015**, *94*, 52. (h) Mück, F. M.; Baus, J. A.; Burschka, C.; Tacke, R. *Chem. Eur. J.* **2016**, *22*, 5830.

(3) (a) Rendler, S.; Oestreich, M. *Synthesis* **2005**, *11*, 1727. (b) Oishi, M. In *Lewis Acids in Organic Synthesis*; Yamamoto, H., Ed.; Wiley-VCH: Weinheim, 2000; Vol. 1, p 355. (c) Dilman, A. D.; Ioffe, S. L. *Chem. Rev.* **2003**, *103*, 733.

(4) Groom, C. R.; Bruno, I. J.; Lightfoot, M. P.; Ward, S. C. *Acta Crystallogr., Sect. B: Struct. Sci.* **2016**, *72*, 171-179.

(5) Rectangular pyramidal and square pyramidal are often used synonymously in the literature.

(6) Tacke, R.; Mühleisen, M.; Lopez-Mras, A. *Z. Anorg. Allg. Chem.* **1995**, *621*, 779.

(7) Bassindale, A. R.; Sohail, M.; Taylor, P. G.; Korlyukov, A. A.; Arkhipov, D. E. *Chem. Commun.* **2010**, *46*, 3274.

(8) (a) Kalikhman, I.; Krivonos, S.; Lameyer, L.; Stalke, D.; Kost, D. *Organometallics* **2001**, *20*, 1053. (b) Kalikhman, K.; Girshberg, O.; Lameyer, L.; Stalke, D.; Kost, D. *J. Am. Chem. Soc.* **2001**, *123*, 4709. (c) Kost, D.; Kingston, V.; Gostevskii, B.; Ellern, A.; Stalke, D.; Walfort, B.; Kalikhman, I. *Organometallics* **2002**, *21*, 2293. (d) Kalikhman, I.; Gostevskii, B.; Girshberg, O.;

Krivonos, S.; Kost, D. *Organometallics* **2002**, *21*, 2551. (e) Kalikhman, I.; Kingston, V.; Gostevskii, B.; Pestunovich, V.; Stalke, D.; Walfort, B.; Kost, D. *Organometallics* **2002**, *21*, 4468. (f) Kost, D.; Gostevskii, B.; Kocher, N.; Stalke, D.; Kalikhman, I. *Angew. Chem. Int. Ed.* **2003**, *42*, 1023. (g) Kalikhman, I.; Gostevskii, B.; Girshberg, O.; Sivaramakrishna, A.; Kocher, N.; Stalke, D.; Kost, D. *J. Organomet. Chem.* **2003**, *686*, 202. (h) Gostevskii, B.; Pestunovich, V.; Kalikhman, I.; Sivaramakrishna, A.; Kocher, N.; Deuerlein, S.; Leusser, D.; Stalke, D.; Kost, D. *Organometallics* **2004**, *23*, 4346. (i) Gostevskii, B.; Silbert, G.; Adear, K.; Sivaramakrishna, A.; Stalke, D.; Deuerlein, S.; Kocher, N.; Voronkov, M. G.; Kalikhman, I.; Kost, D. *Organometallics* **2005**, *24*, 2913. (j) Sivaramakrishna, A.; Kalikhman, I.; Kertsnus, E.; Korlyukov, A. A.; Kost, D. *Organometallics* **2006**, *25*, 3665. (k) Gostevskii, B.; Zamstein, N.; Korlyukov, A. A.; Baukov, Y. I.; Botoshansky, M.; Kaftory, M.; Kocher, N.; Stalke, D.; Kalikhman, I.; Kost, D. *Organometallics* **2006**, *25*, 5416. (l) Jouikov, V.; Gostevskii, B.; Kalikhman, I.; Kost, D. *Organometallics* **2007**, *26*, 5791. (m) Kalikhman, I.; Gostevskii, B.; Sivaramakrishna, A.; Kost, D.; Kocher, N.; Stalke, D. In *Organosilicon Chemistry VI: From Molecules to Materials*; Auner, N., Weis, J., Eds.; VCH, Weinheim, 2005, p 297. (n) Kost, D.; Kalikhman, I. *Acc. Chem. Res.* **2009**, *42*, 303.

(9) (a) Wagler, J.; Gerlach, D.; Roewer, G. *Chem. Heterocyc. Compd.*, **2006**, *42*, 1557. (b) Wächtler, E.; Kämpfe, A.; Krupinski, K.; Gerlach, D.; Kroke, E.; Brendler, E.; Wagler, J. *Z. Naturforsch.* **2014**, *69b*, 1402.

(10) Kämpfe, A.; Brendler, E.; Kroke, E.; Wagler, J. *Chem. Eur. J.* **2014**, *20*, 9409.

(11) (a) Wagler, J.; Böhme, U.; Brendler, E.; Thomas, B.; Goutal, S.; Mayr, H.; Kempf, B.; Remennikov, G. Ya.; Roewer, G. *Inorg. Chim. Acta* **2005**, *358*, 4270. (b) Singh, M. S.; Singh, P. K. *Main Group Met. Chem.* **2000**, *23*, 183. (c) Singh, M. S.; Singh, P. K. *Syn. React. Inorg. Met.* **2003**, *33*, 271. (d) Raju, M. D. *Main Group Met. Chem.* **2009**, *32*, 101. (e) Singh, M. S.; Sharma, T. C.; Singh, P. K. *Synthetic Commun.* **2002**, *32*, 3733.

(12) Baus, J. A.; Burschka, C.; Bertermann, R.; Guerra, C. F.; Bickelhaupt, F. M.; Tacke, R. *Inorg. Chem.* **2013**, *52*, 10664.

(13) (a) Schott, V. G.; Golz, K. *Z. Anorg. Allg. Chem.* **1971**, *383*, 314. (b) Schott, V. G.; Golz, K. *Z. Anorg. Allg. Chem.* **1973**, *399*, 7. (c) Serpone, N.; Hersh, K. A. *J. Organomet. Chem.* **1975**, *84*, 177.

(14) Muetterties, E. L.; Roesky, H.; Wright, C. M. *J. Am. Chem. Soc.* **1966**, *88*, 4856.

(15) Shipov, A. G.; Korlyukov, A. A.; Kramarova, E. P.; Arkhipov, D. E.; Bylikin, S. Yu.; Hunze, F.; Pogozhikh, S. A.; Murasheva, T. P.; Negrebetskii, V. V.; Khrustalev, V. N.;

Ovchinnikov, Yu. E.; Bassindale, A. R.; Taylor, P. G. A.; Baukov, Yu. I. *Russ. J. Gen. Chem.* **2011**, *81*, 2412.

(16) (a) Singh, M. S.; Bhagwat, V. W.; Raju, M. David; Tiwari, S. K. *Ind. J. Chem. A*, **1999**, *38A*, 716. (b) Singh, M. S.; Raju, M. David; Singh, A. K.; Tiwari, S. K. *Main Group Met. Chem.* **1998**, *21*, 643.

(17) Kraft, B. M.; Brennessel, W. W. *Organometallics* **2014**, *33*, 158.

(18) Other organosilicon complexes bearing the OPO ligand are described in Tacke, R.; Burschka, C.; Willeke, M.; Willeke, R. *Eur. J. Inorg. Chem.* **2001**, 1671.

(19) (a) Weiss, A.; Harvey, D. R. *Angew. Chem.* **1964**, *76*, 818. (b) Tacke, R.; Willeke, M.; Penka, M. *Z. Anorg. Allg. Chem.* **2001**, *627*, 1236. (c) Kraft, B. M.; Brennessel, W. W.; Ryan, A. E.; Benjamin, C. E. *Acta Cryst.* **2015**, E71, 1531–1535.

(20) The *cis* arrangement of chelate rings is typical of most other known hexacoordinate Si complexes having monoanionic bidentate ligands. For examples having *trans*-oriented chelates, see refs 8d, 8g, 10 and (a) Hahn, F. E.; Keck, M.; Raymond, K. N. *Inorg. Chem.* **1995**, *34*, 1402. (b) Schley, M.; Wagler, J.; Roewer, G. *Z. Anorg. Allg. Chem.* **2005**, *631*, 2914. (c) Janardan, S.; Suman, P.; Sivaramakrishna, A.; Vijayakrishna, K. *Polyhedron* **2015**, *85*, 34. (d) Aksamentova, T. N.; Chipanina, N. N.; Voronkov, M. G.; Grebneva, E. A.; Albanov, A. I.; Trofimova, O. M.; Mukha, S. A.; Sukhov, B. G. *Russ. J. Gen. Chem.* **2009**, *79*, 98.

(21) For Si*CClN*$_2$*O*$_2$ cores having dissociated chloride, see refs 8a, 8i, 8j and (a) Wagler, J.; Böhme, U.; Brendler, E.; Roewer, G. *Z. Naturforsch.* **2004**, *59b*, 1348.

(22) For hexacoordinate Si*CClN*$_2$*O*$_2$ cores, see ref 9b, ref 10, and (a) Kost, D.; Kalikhman, I.; Krivonos, S.; Stalke, D.; Kottke, T. *J. Am. Chem. Soc.* **1998**, *120*, 4209. (b) Klebe, G.; Qui, D. T. *Acta Crystallogr. C* **1984**, *40*, 476. (c) Kalikhman, I.; Gostevskii, B.; Kertsnus, E.; Botoshansky, M.; Tessier, C. A.; Youngs, W. J.; Deuerlein, S.; Stalke, D.; Kost, D. *Organometallics* **2007**, *26*, 2652. (d) Mozzhukhin, A. O.; Antipin, M. Yu.; Struchkov, Yu. T.; Gostevskii, B. A.; Kalikhman, I. D.; Pestunovich, V. A.; Voronkov, M. G. *Metalloorg. Khim.* **1992**, *5*, 658. (e) Gostevskii, B.; Adear, K.; Sivaramakrishna, A.; Silbert, G.; Stalke, D.; Kocher, N.; Kalikhman, I.; Kost, D. *Chem. Commun.* **2004**, 1644. (f) Kalikhman, I.; Girshberg, O.; Lameyer, L.; Stalke, D.; Kost, D. *Organometallics* **2000**, *19*, 1927.

(23) Complexes **4**, **5**, and **6** exhibit structures with 92.8%, 94.4%, and 92.2% progress, respectively, along the TBP → SP Berry-pseudorotation coordinate. The O—Si—O bond angles in the ideal SP form are 151°. See ref 7 and Holmes, R. R.; Deiters, J. A. *J. Am. Chem. Soc.* **1977**, *99*, 3318.

(24) The directionality of the folding of the aromatic rings toward the apical substituent appears to be general to related Si*CO*$_4$ anionic cores having similar SP geometries. See (a) Tacke, R.; Heermann, J.; Pülm, M.; Gottfried, E. *Monatsh. Chem.* **1999**, *130*, 99. (b) Holmes, R. R.; Day, R. O.; Harland, J. J.; Sau, A. C.; Holmes, J. M. *Organometallics* **1984**, *3*, 341. (c) Holmes, R. R.; Day, R. O.; Chandrasekhar, V.; Harland, J. J.; Holmes, J. M. *Inorg. Chem.* **1985**, *24*, 2016. (d) Holmes, R. R.; Day, R. O.; Chandrasekhar, V.; Holmes, J. M. *Inorg. Chem.* **1985**, *24*, 2009. (e) Tacke, R.; Lopez-Mras, A.; Sheldrick, W. S.; Sebald, A. *Z. Anorg. Allg. Chem.* **1993**, *619*, 347. (f) Swamy, K. C. K.; Chandrasekhar, V.; Harland, J. J.; Holmes, J. M.; Day, R. O.; Holmes, R. R. *J. Am. Chem. Soc.* **1990**, *112*, 2341. (g) Mercado, R.-M. L.; Chandrasekaran, A.; Day, R. O.; Holmes, R. R. *Organometallics* **1999**, *18*, 1686. (h) Tacke, R.; Lopez-Mras, A.; Sperlich, J.; Strohmann, C.; Kuhs, W. F.; Mattern, G.; Sebald, A. *Chem. Ber.* **1993**, *126*, 851. (i) Strohmann, C.; Tacke, R.; Mattern, G.; Kuhs, W. F. *J. Organomet. Chem.* **1991**, *403*, 63.

(25) A lower quality crystal of **4**·2$CDCl_3$ (see the Supporting Information), exhibited the same SP geometry in the two independent molecules of the unit cell. The Si···Cl distances are 3.521(3) and 3.524(3) Å, and each chloride ion has a strong intermolecular H-bonding contact with a $CDCl_3$ molecule ($d_{H\cdots Cl}$ = 2.35 Å; ∠C—H···Cl = 174.2° and $d_{H\cdots Cl}$ = 2.40 Å; ∠C—H···Cl = 168.4°) among three additional H-bonding contacts with neighboring cations of **4**.

(26) Brendler, E.; Heine, T.; Hill, A. F.; Wagler, J. *Z. Anorg. Allg. Chem.* **2009**, *635*, 1300.

(27) Despite OPO ligand disorder in complexes **1-6**, the symmetry of the π-system is expected to allow a reasonable comparison of these particular structural features.

(28) Kocher, N.; Henn, J.; Gostevskii, B.; Kost, D.; Kalikhman, I.; Engels, B.; Stalke, D. *J. Am. Chem. Soc.* **2004**, *126*, 5563.

(29) In ref 9b, large Si-C-C angles are also observed in $BnSiCl_3$ (113.6°) and Bn_2SiCl_2 (114.1° and 115.0°) and were ascribed to sterics arising from intramolecular repulsion between chlorine and an *ortho*-hydrogen atom of the benzyl group. Structures of $BnSi(oxinate)_2Cl$ and $Bn_2Si(oxinate)_2$ also have wide Si-C-C angles.

(30) Presumably due to fluxional processes, the ^{29}Si NMR resonance for complex **5** was very weak and that of **6** could not be found. A small downfield shift (~0.5 ppm) was observed upon increasing the temperature from 25 °C to 60 °C in **2** and **3**, but the signal could not be found at 60 °C for the other complexes.

(31) Helmer, B. J.; West, R.; Corriu, R. J. P.; Poirier, M.; Royo, G.; de Saxce, A. *J. Organomet. Chem.* **1983**, *251*, 295.

(32) Although two isomers are evident, double ^{29}Si NMR resonances were not resolved.

(33) Exchange of chloride for triflate by this method has also been reported in (a) Belzner, J.; Schär, D.; Kneisel, B. O.; Herbst-Irmer, R. *Organometallics* **1995**, *14*, 1840. (b) Berlekamp, U.-H.; Jutzi, P.; Mix, A.; Neumann, B.; Stammler, H.-G.; Schoeller, W. W. *Angew. Chem., Int. Ed.* **1999**, *38*, 2048.

(34) These reactions could not be done in NMR tubes in DMSO-d_6 as the byproduct, Me_3SiCl, was found to react with DMSO to form unidentified products. The reactions of $SiCl_4$ and $RSiF_3$ complexes with DMSO are known. See (a) George, K.; Hector, A. L.; Levason, W.; Reid, G.; Sanderson, G.; Webster, M.; Zhang, W. *Dalton Trans.* **2011**, *40*, 1584. (b) Voronkov, M. G.; Boyarkina, E. V.; Gavrilova, G. A.; Basenko, S. V. *Russ. J. Gen. Chem.* **2001**, *71*, 1865.

(35) Complex **4** was chosen due to its methyl protons in close proximity to the silicon center. The same effect on chemical shifts was also demonstrated with DMSO and the CH_2 resonance of complex **3**. Due to their very limited solubility in $CDCl_3$ and CD_3CN, only their ^1H NMR spectra could be obtained with an adequate signal. It was possible to identify the DMSO peak in the ^{13}C NMR spectrum of **4**, but not the apparently broadened $SiCH_3$ resonance.

(36) The first equivalent of DMSO produced an upfield shift (Δ = 1.0 ppm) of the ^{13}C NMR resonance of DMSO and gradually moved toward its native position with increasing concentration.

(37) Similar behavior is observed in $SiF_4 \cdot 2DMSO$ where the DMSO proton resonance is shifted ~0.3 ppm downfield from its native position in CD_3CN. See: Lermontov, S. A.; Malkova, A. N.; Lermontova, E. Kh.; Churakov, A. V. *Phosphorus, Sulfur, and Silicon* **2011**, *186*, 178.

(38) Cella, J. A.; Cargioli, J. D.; Williams, E. A. *J. Organomet. Chem.* **1980**, *186*, 13.

(39) (a) Kost, D.; Kalikhman, I.; Raban, M. *J. Am. Chem. Soc.* **1995**, *117*, 11512. (b) Kalikhman, I.; Krivonos, S.; Stalke, D.; Kottke, T.; Kost, D. *Organometallics* **1997**, *16*, 3255.

(40) Green, M. L. H.; Wong, L. L.; Sella, A. *Organometallics* **1992**, *11*, 2660.

(41) Dannappel, O.; Tacke, R. In *Organosilicon Chemistry II: From Molecules to Materials*; Auner, N.;,Weis, J., Eds.;VCH, Weinheim, 1996, p 453.

(42) (a) Serpone, N.; Bickley, D. G. *Prog. Inorg. Chem.* **1972**, *17*, 391. (b) Corriu, R. J. P.; Kpoton, A.; Poirier, M.; Royo, G.; Corey, J. Y. *J. Organomet. Chem.* **1984**, *277*, C25. (c) Negrebetsky, V. V.; Tandura, S. N.; Baukov, Yu. I. *Russ. Chem. Rev.* **2009**, *78*, 21. (d) Couzijn, E. P. A.; Schakel, M.; de Kanter, F. J. J.; Ehlers, A. W.; Lutz, M.; Spek, A. L.; Lammertsma, K. *Angew. Chem., Int. Ed.*, **2004**, *43*, 3440. (e) Couzijn, E. P. A.; van den Engel, D. W. F.; Slootweg, J. C.; de Kanter, F. J. J.; Ehlers, A. W.; Schakel, M.; Lammertsma, K. *J. Am. Chem. Soc.* **2009**, *131*, 3741. (f) Couzijn, E. P. A.; Slootweg, J. C.; Ehlers, A. W.; Lammertsma, K. *J. Am. Chem. Soc.* **2010**, *132*, 18127.

(43) *APEX3*, version 2015.9-0; Bruker AXS: Madison, WI, 2015.

(44) Sheldrick, G. M. *SADABS*, version 2014/5; *J. Appl. Cryst.* **2015**, *48*, 3.

(45) *SAINT*, version 8.34A; Bruker AXS: Madison, WI, 2013.

(46) Burla, M. C.; Caliandro, R.; Camalli, M.; Carrozzini, B.; Cascarano, G. L.; Giacovazzo, C.; Mallamo, M.; Mazzone, A.; Polidori, G.; Spagna, R. *SIR2011: A new package for crystal structure determination and refinement*, version 1.0; Istituto di Cristallografia: Bari, Italy, 2012.

(47) Sheldrick, G. M. *SHELXT-2014/5*; University of Göttingen: Göttingen, Germany, 2014.

(48) Sheldrick, G. M. *SHELXL-2014/7*; *Acta. Cryst.* **2015**, *C71*, 3.

For Table of Contents Only: